INHOMOGENEOUS DECONVOLUTION IN A BIOLOGICAL IMAGES CONTEXT

A.Ogier, T. Dorval, A. Genovesio

Image Mining Group
Institut Pasteur Korea
39-1, Hawolgok-dong, Seongbuk-gu, Seoul, 136-791, Korea

ABSTRACT

In this paper we present a new framework for correcting partially out-of-focus biological images. To evaluate depth variation, our method extracts similar objects of interest over the image. The depth is based on a defocus value computation for each salient point. We use an iterative algorithm to convert each defocus value into a Gaussian standard deviation. These measures are then interpolated over the whole image using thin plate spline transform, providing a regularized map. This array provides, for every spatial position, an evaluation of the standard deviation used in the final step for an inhomogeneous deconvolution based on the Richardson-Lucy algorithm. Experiments on real and simulated images validate the accuracy of such a method compare to traditional shift invariant deconvolution approaches.

Index Terms— Deconvolution, microscopy, image processing, image restoration, image enhancement.

1. INTRODUCTION

The standard formulation for a shift invariant blurring phenomenon for an optical system is describe by the following equation :

$$g(x,y) = \mathcal{P}\big((h * f)(x,y)\big) + \eta. \quad (1)$$

Here, $h(x,y)$ is the blur function, $f(x,y)$ the original image, $\mathcal{P}$ the Poisson distribution, η is typically the acquisition noise that follows a Gaussian distribution, $g(x,y)$ the observed image and $*$ the convolution operator. In this paper, the blur function is considered as spatially variant. Then, equation (1) takes the form:

$$g(x,y) = \mathcal{P}\big((h_{(i,j)} * f)(x,y)\big) + \eta. \quad (2)$$

Now, the function h can change along the image. The out-of-focus blurring process is modeled by a symmetrical Gaussian convolution $\sim \mathcal{N}(0, \sigma_{i,j})$. For more explanation concerning the physical foundations of this assumption, the reader can refer to [1, 2]. We need to estimate the standard deviation map $\hat{\sigma}_{i,j}$ of the Gaussian function $h_{(i,j)}(x,y)$ from information contained in the image $g(x,y)$. 2D image deconvolution is an especially ill-posed problem, particularly if we consider that the Point Spread Function (PSF) may vary over the image. To overcome this drawback we have to constrain the solution by including additional assumptions to the process [3, 4, 5].

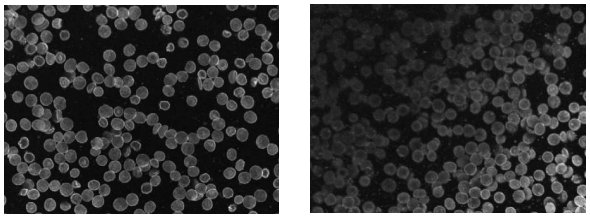

(a) **(b)**

Fig. 1. **Schematic representation of the defocusing phenomenon. In figure (a) the biological matter is well located in the focal plane. In figure (b) the biological objects are out-of-focus, projecting a corrupted image in the image plane.**

Our first assumption consists in adding a smoothness constraint to the solution. It is a very common regularity constraint [5] and is realized here by using a thinplate spline interpolation between relevant estimated $\hat{\sigma}_{i,j}(x,y)$ values.

We also assume that a same biological object is spread over the image. This situation is typical in biological screening image context (see figures 1, 6, 2 & 5). Of course these objects may be subject to different blurs due to their depth (see figure 1). We use these entities as references in order to determinate the focus measures over the image.

In this paper we split the framework in three distinct parts: (i)the defocusing trend quantification, (ii) the Gaussian kernels estimation and (iii) the deconvolution process.

2. DEFOCUSING QUANTIFICATION

The first step of our framework consists in estimating the amount of blur present in the image. In the defocus estimation literature, a recent paper [6] compares several focus measures and shows that Sum-Modified-Laplacian (SML) provides better performances[1]. Thus we base our blur estimation upon the

[1] http://homepage.ntu.edu.tw/ p94922001/FocusStudy.htm

use of this operator applied on a small neighborhood N. It is described as follows [1]:

$$F(i,j) = \sum_{x=i-N}^{i+N} \sum_{y=j-N}^{j+N} L_{Mod}(x,y), \qquad (3)$$

where

$$\begin{aligned} L_{Mod}(x,y) &= |2g(x,y) - g(x-\Delta x, y) - g(x+\Delta x, y)| \\ &+ |2g(x,y) - g(x, y-\Delta y) - g(x, y+\Delta y)|. \end{aligned}$$

The figure 2(b) displays the SML map with $N = 3$. SML measures high frequencies (details) and, as we can see in figure 2(b), the object edges themselves affect the relevance of this estimation. To overcome this drawback, we propose to calculate the SML criterion only on similar objects as defined in section 1.

In many cases, and after a Gaussian filtering process, entities in biological images can be considered as an extrema in a topographic sense. Wilson *et al.* in [7] differentiate many topographic classes to the mean H and Gaussian K curvatures (rotational invariant) of the surface. Using this detection method we extract the local maxima by defining d_{min} as the minimum distance between two detected points. d_{min} is directly related to the number of extracted points $N_{salient}$. The choice of this distance depends of the number of biological objects present in the image. $N_{salient}$ must be lower than the cardinal of biological objects to avoid false detection. The figure 2(a) shows the result of a typical relevant detection (red crosses represent the list $\mathbf{F}_{salient}$ of salient points, with $\#\mathbf{F}_{salient} = N_{salient}$).

3. SHIFT VARIANT BLUR ESTIMATION

We consider that the highest value of SML gives us the reference focus in the image. At this position the standard deviation σ_0 of the PSF is given by an *a priori* knowledge of the user, depending of the optical system considered.

Due to the non linearity of SML and the complexity of the images, it is not obvious to find a relation, or function, $\varphi \mid \sigma = \varphi(F_{salient})$ between the SML values and σ (see figure 3). Thus, to estimate for each SML value the corresponding $\hat{\sigma}$ we apply the algorithm 1.

We compute the SML value of the reference object iteratively convolved by ϵ. This resulting value is compared to all the remaining SML values of the $\mathbf{F}_{salient}$ list. If a value matches, the considered point is removed from the list and the corresponding $\hat{\sigma}$ is assigned (see figures 3(a)).

The out of focus phenomenon is assumed to be smooth (without discontinuities) consequently we can apply a spline thin plate interpolation in order to reconstruct the $\hat{\sigma}_{i,j}$ map for any points of the image. The result of this interpolation can be seen in figure 4(c).

Algorithm 1 from SML to standard deviation

$\sigma \Leftarrow \sigma_0$
$F_{max} \Leftarrow max(List[F_{salient}])$
while $List[F_{salient}] \neq \emptyset$ **do**
  $I_\sigma \Leftarrow h_\sigma * I(x_{F_{max}}; y_{F_{max}})$
  $F_\sigma \Leftarrow \Delta I_\sigma(x_{F_{min}}; y_{F_{min}})$
  for $i = 1$ to $\sharp(List[F_{salient}])$ **do**
    if $F_i \geq F_\sigma$ **then**
      Remove F_i from $List[F_{salient}]$
      Add I_σ to $List[I_{salient}]$
    end if
  end for
  $\sigma \Leftarrow \sigma + \epsilon$
end while

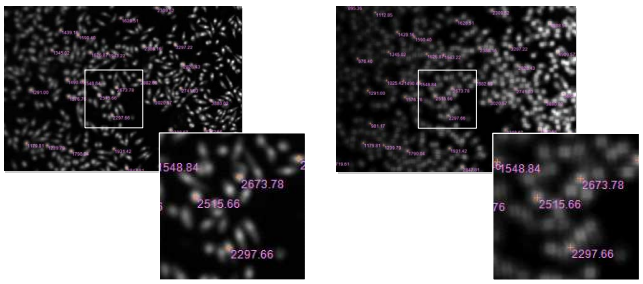

(a) **(b)**

Fig. 2. **Points of interest and associated SML values represented respectively on: (a) the natural image and (b) the corresponding SML map.**

4. INHOMOGENEOUS DECONVOLUTION

Our images are degraded by out-of-focus blur and, in optical microscopy, are subject to Poisson noise (see equation (2)). Among deconvolution algorithms existing in the literature, the Richardson-Lucy [8] which computes a maximum likelihood estimation adapted to Poisson statistics, is particularly well suited for our aim. It leads to minimize the following functional [9]:

$$E(f) = \iint [(h * f)(x,y) - g(x,y)\log(h * f)(x,y)]dxdy.$$

This minimization process, using the multiplicative algorithm version, can be written as:

$$f_{k+1}(x,y) = f_k(x,y)\left[h(x,y) * \frac{g(x,y)}{(h * f_k)(x,y)}\right],$$

when $h(x,y)$ is a symmetric Gaussian kernel. The constant convolution kernel $h(x,y)$ can be easily substituted by a space variant one, leading to:

$$f_{k+1}(x,y) = f_k(x,y)\left[h_{(i,j)}(x,y) * \frac{g(x,y)}{(h_{(i,j)} * f_k)(x,y)}\right].$$

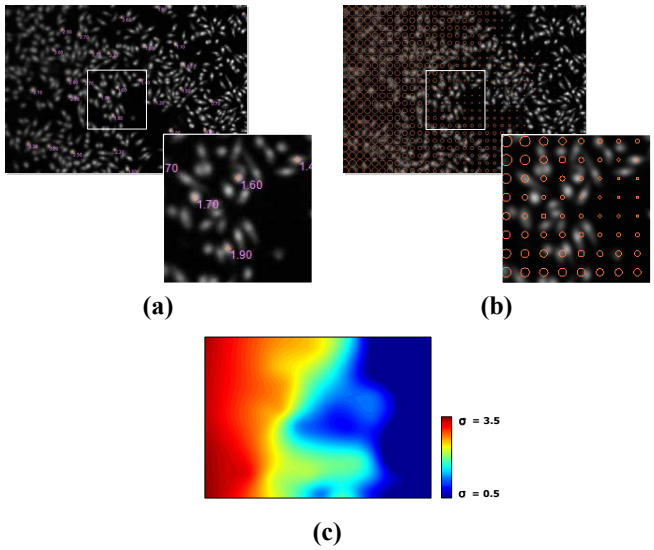

Fig. 3. **Three different representations of the $\hat{\sigma}_{i,j}$ values: (a) the numerical values attached to each point of interest, (b) spatially regular superimposed of the isotropic kernel of radius $\hat{\sigma}_{i,j}$ and (c) the final $\hat{\sigma}_{i,j}$ map computed using the thinplate interpolation.**

This inhomogeneous deconvolution is driven by the interpolated map of $\hat{\sigma}_{i,j}$ (see figure 3(c)). The figure 3(b) illustrates the Gaussian standard deviation by drawing some circles of radius $r = \hat{\sigma}_{i,j}$.

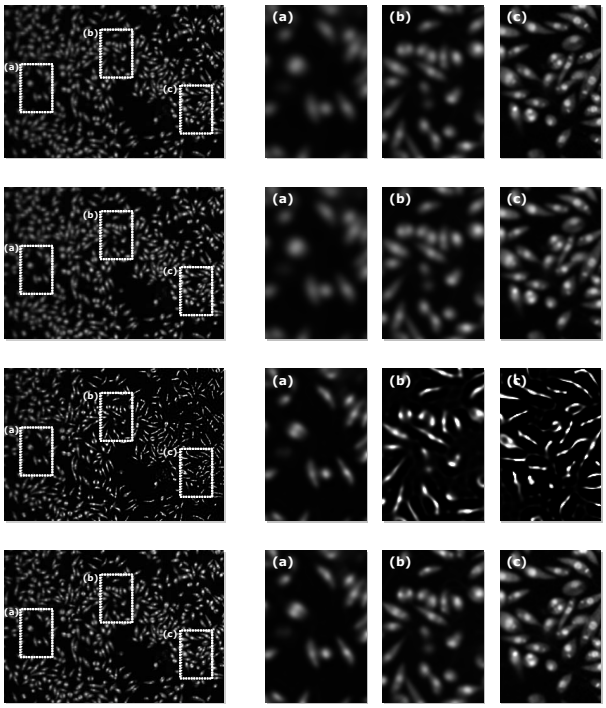

Fig. 4. **This figure displays an image and three selected regions of interest. Top: Corrupted image. Second row: Result of homogeneous deconvolution with $\sigma = 1$. Third row: Result of homogeneous deconvolution with $\sigma = 3.2$. Bottom: Our inhomogeneous deconvolution using $\hat{\sigma}_{i,j}$ (see figure 3).**

5. RESULTS

Validation of our method is a non obvious task since usually, for real images, we don't possess ground truth. Despite this, for the first evaluation process, we simulate partially out-of-focus images by inhomogeneously convolve natural acquisitions. The $\sigma_{i,j}$ map is a random coefficients 2D Legendre orthogonal polynomial. We then, compute the $\hat{\sigma}_{i,j}$ for different kind of biological images (red blood cells, parasites...). The results are displayed on figure 6 and 5. Whatever the assay is, the estimated standard deviation maps respect the trend and the dynamic of the original one.

We also propose a result based on the comparison between our algorithm and the traditional homogeneous Richardson-Lucy deconvolution for two different $h(x, y)$ (see second and third row of the figure 4) for a natural image. Thus, as expected, the under estimation of the kernel standard deviation leads to a very weak enhancement of the image (see figures 4 (a) & (b) second row). In the other hand, the over estimation considerably damages the image (see figures 4 (b) & (c) third row). Using our framework allows an accurate deconvolution whatever the spatial position is (see figure 4 last row).

6. CONCLUSION AND FUTURE WORKS

This paper presents a 2D inhomogeneous deconvolution algorithm using jointly a measure of the sharpness (blur amount) on detected salient points and also a spatial variant deconvolution based on Richardson Lucy. We apply the algorithm on simulated images and verify the well founded of our assumptions. Actually, the values obtained are very close from the ground truth and allow an accurate deconvolution. On natural image, we qualitatively demonstrate that inhomogeneous deconvolution outperforms the standard one.
Nowadays, we are working on the detection part to provide an extended version of this algorithm in order to deconvolve images containing many kind of objects.

7. ACKNOWLEDGMENT

The authors thank Hyun Rim Oh, Min-Je Ku, Gyongseon Yang, Lucio Freitas-Junior and his Systems Biology of Pathogens group from Institut Pasteur Korea for providing valuable microscopic images.

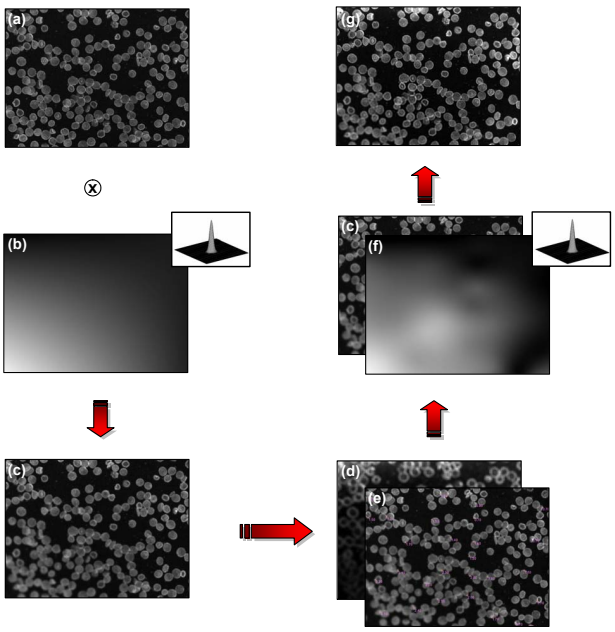

Fig. 5. **(a) focused image. (b) Synthetic generated $\sigma(x, y)$ map of the Gaussian function standard deviation. (c) Inhomogeneous convolution result. (e) SML values for the detected point of interest extract from the (d) SML map. (f) Thin plate interpolated map $\widetilde{\sigma}(x, y)$. (g) Inhomogeneous deconvolution of (c) based on the (f) map.**

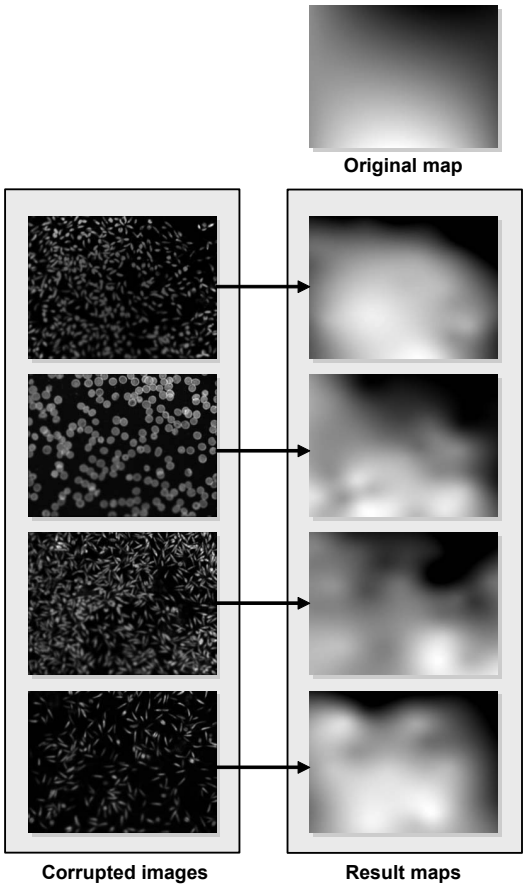

Fig. 6. **Estimated $\hat{\sigma}_{i,j}$ maps of 4 artificially corrupted images using the same $\sigma_{i,j}$ for the homogeneous convolution. Whatever the biological assay is, the results are relevant and thus allow an accurate deconvolution process.**

8. REFERENCES

[1] S.K. Nayar and Y. Nakagawa, "Shape from focus," *IEEE Transactions on Pattern Analysis and Machine Intelligence*, vol. 16, no. 8, pp. 824–831, August 1994.

[2] F. Rooms, M.Ronse, A. Pizurica, and W. Philips, "Psf estimation with applications in autofocus and image restoration," in *3rd IEEE Benelux Signal Processing Symposium*, 2002.

[3] T. R. Lauer, "Deconvolution with a spatially-variant psf," in *Proceedings of the SPIE Astronomical Data Analysis II*, 2002, pp. 167–173.

[4] L. Bar, N.A. Sochen, and N. Kiryati, "Restoration of images with piecewise space-variant blur," in *Scale Space and Variational Methods in Computer Vision (SSVM'07)*, 2007, pp. 533–544.

[5] M. Blume, D. Zikic, W. Wein, and N. Navab, "A new general method for blind shift-variant deconvolution of biomedical images," in *Proceedings of the 10th conference on Medical Image Computing and Computer-Assisted Interventation (MICCAI'07)*, 2007, pp. 743–750.

[6] W. Huang and Z. Jing, "Evaluation of focus measures in multi-focus image fusion," *Pattern recognition letters*, vol. 28, pp. 493–500, 2007.

[7] R. C. Wilson and E.R. Hancock, "Consistent topographic surface labelling," *Pattern Recognition Letters*, vol. 32, pp. 1211–1223, 1999.

[8] W.H. Richardson, "Bayesian-based iterative method of image restoration," *Journal of the Optical Society of America*, vol. 62, pp. 55–59, 1972.

[9] N. Dey, L. Blanc-Fraud, C. Zimmer, Z. Kam, P. Roux, J.C. Olivo-Marin, and J. Zerubia, "Richardson-lucy algorithm with total variation regularization for 3d confocal microscope deconvolution," *Microscopy Research Technique*, vol. 69, pp. 260–266, 2006.